8 Dynamical Mean-Field Theory for Correlated Electrons with Disorder

Krzysztof Byczuk
Institute of Theoretical Physics, University of Warsaw
Pasteura 5, 02-093 Warszawa, Poland

Contents

E. Pavarini, E. Koch, A. Lichtenstein, and D. Vollhardt (eds.)
Understanding Correlated Materials with DMFT
Modeling and Simulation Vol. 15
Forschungszentrum Jülich, 2025, ISBN 978-3-95806-813-1
http://www.cond-mat.de/events/correl25

1 Introduction

For a classical observer the empty space, i.e., the vacuum, is perfectly regular with perfect translational and rotational symmetry. The vacuum is homogeneous and isotropic. Inserting particles into the vacuum breaks this perfect symmetry. However, if the particles are arranged in a regular fashion, there is still some symmetry in the system. For example, in case of perfect crystals, infinitely large, there is a discrete translational and a point group symmetry. In case of a single molecule or a cluster of molecules a discrete point group symmetry might be present. In the fascinating word of quasicrystals, the infinitely large system is not translationally symmetric but a certain point group symmetry is still present. These systems are regular, predictable and often exactly tractable in a mathematical description [1]. These regularities have been an inspiration for artists and architects for centuries around the word.

If there is a regularity in the nature there must be an irregularity as well [2]. Indeed, investigating systems very often one finds irregularities in the arrangements of atoms or molecules [3]. The hardest system in the nature, a diamond, is an arrangement of carbon atoms in a cube repeated infinitely many times in space. The perfect diamond is transparent and colorless insulator. If some randomly chosen carbons are replaced by nitrogens the diamond becomes a conductor, and is used in electronics, e.g., in transistors. When randomly substituting boron atoms for carbons a diamond becomes blueish but randomly deforming the perfect bond structure makes the crystal reddish. These defects in a diamond are welcome, making the crystal more rare and more visually intriguing and increase its price on the stock as well.

Irregularities are typically unrepeatable. But are present in most real physical systems. Their presence changes properties of the systems, sometimes along our intention but sometimes against it. As theoretical physicists we want to learn how to describe irregular systems mathematically [4].

In this lecture notes we will focus on some narrow aspects of irregular systems, namely on correlated electron (fermion) systems, and present how to combine the well know **dynamical mean-field theory** (DMFT) with mathematical theories tackling randomness. We start with defining various types of disordered systems on a model level within tight-binding approximations and discuss mathematical/statistical tools to describe such systems. We introduce systems with a binary disorder as well as with a continuous disorder. Both represent different situations in solid state physics. Next we will discuss a combination of the dynamical mean-field theory with the **coherent potential approximation** (CPA) for disordered systems. These are two *dynamical* mean-field type approximations to finite dimensional systems and are exact in infinite dimensions. As we will emphasize, both DMFT and CPA treats correlations and disorder on equal footing. We present two surprising results concerning the Curie temperature and the Mott-Hubbard **metal-insulator transition** (MIT) at fractional filling in the binary alloy systems. Further we will introduce the Anderson transition, a different kind of MIT triggered by randomness in the system. The DMFT is extended in such manner that the most probable realization is taken into account. This is a **typical medium theory** (TMT) which is combined with the DMFT, instead of the CPA, and predicts phase diagrams with different metallic and insulating phases in correlated electron models, such as Hubbard and Falicov-Kimball ones. We will end with some short discussion of other developments where DMFT is used for disordered electrons, fermions and bosons, and comment on present approaches toward the many-body localization.

2 Disordered systems, random variables, averages

2.1 Models of disorder electrons

We shall consider model systems describing electrons moving in irregular crystals. Following the pioneering work of Anderson [5] we use the standard model, today known as the Anderson model, represented by a second-quantized Hamiltonian

$$\hat{H}_{\mathrm{A}} = \sum_{i\sigma} \varepsilon_i \, \hat{a}^\dagger_{i\sigma} \hat{a}_{i\sigma} + \sum_{ij\sigma} t_{ij} \, \hat{a}^\dagger_{i\sigma} \hat{a}_{j\sigma} \, , \tag{1}$$

where $\hat{a}_{i\sigma}$ ($\hat{a}^\dagger_{i\sigma}$) is an annihilation (creation) operator of an electron at lattice site $\mathbf{R}_i$, in a one particle Wannier basis, and with a spin $\sigma = \pm 1/2$ (in units with $\hbar$=1). Here the creation and annihilation operators obey standard anticommutation relations. The first term represents on-site energies ε_i and the second one a hopping t_{ij} of electrons between different lattice sites. It is the simplest tight-binding model describing electrons on a lattice. The interaction between electrons is absent for the moment.

For a perfectly regular uniform lattice system the on-site energies are the same on all lattice sites, i.e., $\varepsilon_i = \varepsilon$, and the hopping amplitudes t_{ij} are the same for the sites with the same distance $\|\mathbf{R}_i - \mathbf{R}_j\|$. For irregular, non-uniform systems the on-site energy may depend on the lattice site. For example, it can be a random number or it can be different but changed in a regular fashion. For example, in the presence of a uniform electric field along a one dimensional chain, the on-site energies are $\varepsilon_i = aE_0 i$, where a is a lattice constant and E_0 is an electric field intensity. In the following we are interested in cases where ε_i are random variables. Typically it is assumed that the probability distribution function factorizes and the random variables ε_i are independent

$$P(\varepsilon_1, ..., \varepsilon_{N_L}) = \prod_{i=1}^{N_L} p(\varepsilon_i), \tag{2}$$

where N_L is the number of lattice sites. In the original Anderson model [5] the hopping part was assumed to be regular. Nevertheless, one can extend the model by assuming that t_{ij} are random variables drawn from a certain probability distribution function. In the following we assume that any irregularity and randomness in the system appears due to random on-site energies ε_i.

The Anderson model (1) does not include any interaction between electrons. The simplest way to add an interaction is to write a Hubbard like Hamiltonian with the random on-site energies

$$\hat{H}_{\mathrm{AH}} = \sum_{i\sigma} \varepsilon_i \, \hat{n}_{i\sigma} + \sum_{ij\sigma} t_{ij} \, \hat{a}^\dagger_{i\sigma} \hat{a}_{j\sigma} + \sum_{i} U_i \, \hat{n}_{i\uparrow} \hat{n}_{i\downarrow}, \tag{3}$$

where $\hat{n}_{i\sigma} = \hat{a}^{\dagger}_{i\sigma}\hat{a}_{i\sigma}$ is the particle number operator and the projection of the spin is denoted by $\uparrow$ ($\downarrow$) symbols. This Anderson-Hubbard (AH) model describes itinerant electrons on a lattice and interacting when two fermions with opposite spins are occupying the same lattice site. The energy penalty $U_i > 0$ again can be a random variable, although in the Hubbard model and in the following notes it is assumed to be uniform, the same on all sites, $U_i = U$.
Another model with interacting fermions is the Falicov-Kimball one, a simplified version of the Hubbard model with particles with one spin projection immobile. The Anderson-Falicov-Kimball (AFK) Hamiltonian reads

$$\hat{H}_{\mathrm{AFK}} = \sum_i \varepsilon_i \, \hat{n}_i + \sum_{ij\sigma} t_{ij} \, \hat{e}^{\dagger}_i \hat{e}_j + \sum_i U_i \, \hat{n}_i \hat{f}^{\dagger}_i \hat{f}_i + \varepsilon_f \sum_i \hat{f}^{\dagger}_i \hat{f}_i, \tag{4}$$

where $\hat{n}_i = \hat{e}^{\dagger}_i \hat{e}_i$ is the particle number operator for itinerant spinless fermions and $\hat{f}_i$ ($\hat{f}^{\dagger}_i$) are annihilation (creation) fermion operators for immobile particles with on-site energy ε_f.

2.2 Average over disorder, most probable value

Imagine a system, described by one of the above Hamiltonian, with given and fixed on-site energies $\{\varepsilon_i\}_{i=1,\ldots,N_L}$. If we solve it exactly we can get information, for example, on thermodynamics of the system. The grand-canonical partition function $\Xi(T, N_L, \mu; \{\varepsilon_i\}) = \mathrm{Tr} e^{-\beta(\hat{H}-\mu\hat{N})}$, where μ is the chemical potential, $\beta = 1/k_B T$ is the inverse of temperature and k_B is the Boltzmann constant, will depend on particular realization of the on-site energies $\{\varepsilon_i\}$. The grand-canonical thermodynamic potential $\Omega(T, N_L, \mu; \{\varepsilon_i\}) = -k_B T \ln \Xi(T, N_L, \mu; \{\varepsilon_i\})$ and all other thermodynamic functions will be system dependent as well.
To overcome this difficulty, and to get some reliable information about the considered system we take a statistical average over $\{\varepsilon_i\}$. In most situations it is the *arithmetic average*, i.e., for an observable $O(\{\varepsilon_i\})$ we determine

$$\big\langle O(\{\varepsilon_i\}) \big\rangle = \int \prod_{i=1}^{N_L} O(\{\varepsilon_i\}) \, p(\varepsilon_i) \, d\varepsilon_i \tag{5}$$

according to the central limit theorem [6], for infinitely many ($N_L \to \infty$), independent random variables $\{\varepsilon_i\}$. It is a well founded approach for systems which are self-averaging. It means that the sample-to-sample fluctuations

$$\Delta_{N_L}(O) = \frac{\langle O^2 \rangle - \langle O \rangle^2}{\langle O \rangle^2} \tag{6}$$

vanish when $N_L \to \infty$.
In taking an average there are two possibilities, one can take the average of the grand-canonical partition function $\big\langle \Xi(T, N_L, \mu; \{\varepsilon_i\}) \big\rangle$. This situation is called an *annealed disorder*. Another option is to average a physical quantity, like the grand-canonical thermodynamic potential $\big\langle \Omega(T, N_L, \mu; \{\varepsilon_i\} \big\rangle$. This case is named a *quenched disorder* [7]. Unless it is specified otherwise, we will consider here only a quenched type of the disorder.

In nature most systems are self-averaging. Then the ergodic hypothesis is valid and we can use a standard statistical mechanics and arithmetic averaging over the disorder to study such systems in equilibrium. The early work of Anderson [5] put attention to non-ergodic systems, where the concept of statistical averaging does not hold. Anderson described the situation, where in a disordered system the one-particle wave function is localized in a finite subspace of the system. Then, in the dynamical unitary evolution, the quantum system cannot penetrate the whole phase space and cannot probe all possible disorder realizations. Such a system is named an *Anderson insulator*. The ergodic hypothesis cannot be applied and sample-to-sample fluctuations are finite even in the thermodynamic limit. To describe mathematically such non-self-averaging systems we need to focus on the *most probable values* of observables studied on them. This is a *typical* behavior of the system and the one expected to occur in practice.
The prediction of the most probable behavior is difficult. It requires the whole histogram or the whole probability distribution function for a give observable. It requires to solve the Hamiltonian for very many realization of the disorder. For noninteracting models it is demanding but possible, e.g. [8]. For interacting models in large systems it is challenging even today to get good statistics.
Therefore we take a different approach and use a different way of statistical averaging over disorder. We will use a *geometric average* which belongs to generalized means in the probability theory.

2.3 Generalized mean

Consider a single random variable y and a function $f = f(y)$, which is invertible, i.e., $f^{-1}(y)$ exists. The generalized f-mean (average) is defined as

$$\langle y \rangle_f = f^{-1}\big(\langle f(y) \rangle\big), \tag{7}$$

where the average inside is the arithmetic average $\big\langle f(y)\big\rangle = \int dy\, f(y)\, p(y)$ with the probability distribution function $p(y)$ [9]. The f-mean satisfies the usual axioms, required to hold for any useful mean in mathematics [9]. In particular, if we select $f(y) = \ln y$, such an f-mean is the geometric mean or geometric average, i.e.

$$\langle y \rangle_{\ln} = e^{\langle \ln y \rangle}. \tag{8}$$

The popular average in mathematics is the Hölder mean, where $f(y) = y^p$ and p is a number. This Hölder, or p-mean

$$\langle y \rangle_p = \left[\int dy\, y^p\, p(y)\right]^{\frac{1}{p}} \tag{9}$$

is parametrized by a single number p. Like the arithmetic mean, the Hölder mean is a homogeneous function of y and has a block property, i.e., $\langle xy \rangle_p = \langle x \rangle_p \langle y \rangle_p$ if x and y are independent random variables. In particular, if $p{=}-\infty$ this mean gives the possible minimum of y. Other choices, $p{=}-1$ gives a *harmonic mean*, $p{=}0$ gives the geometric mean, $p{=}1$ gives the arithmetic mean, $p{=}2$ gives a *quadratic mean*, and $p{=}\infty$ gives the possible maximum of y.

Which mean gives the best approximation, in particular when the disorder is very strong and drives the system far from the self-averaging limit, is a matter of investigation. For example, many biological and social processes are modeled by the log-normal probability distribution function, for which the geometric average gives the most probable value of the random variable [10, 11]. The same is also true for conductors in series with random resistances.

3 Real-space dynamical mean-field theory

The coherent potential approximation was formulated in 1960's [12], and much earlier than the dynamical mean-field theory, developed in 1990's [13]. However, there are many similarities in these two approaches and, in fact, for correlated electrons models with local disorder the CPA and the DMFT are combined within a singe theoretical approach.

A common denominator between CPA and DMFT is that both are local theories, with local self-energies, depending only on frequencies, and they are playing the roles of the mean-fields. Since they are frequency dependent, the name dynamical mean-field comes. Both theories are comprehensive, thermodynamically consistent and conserving in the Kadanoff-Baym sense [14]. Finally, both are exact in the infinite dimensional limit, or equivalently, in systems with infinite number of nearest neighbors on the lattice [15].

The derivation of the DMFT from the high dimensional perspective was discussed in the Jülich lecture series earlier [16–19] and we do not want to repeat it here. Instead, we offer a straightforward presentation how to use the DMFT for lattice systems with inhomogeneous potentials or random impurities.

The main idea hidden behind the DMFT and the CPA approaches is the mapping of a lattice system, homogeneous or inhomogeneous, onto a local impurity (site) problem, where the impurity (site) is coupled to an effective bath. This bath, like a mean-field, mimics the properties of the rest of the lattice on average.

We consider the Anderson-Hubbard model (3) now. There are various formulations, but the most canonical one and useful for our lecture is the approach where the zero-dimensional single site problem, representing the site i-th, is given by a **single-impurity Anderson model** (SIAM) with the Hamiltonian

$$\hat{H}^{(i)}_{\mathrm{SIAM}} = \varepsilon_i \sum_{\sigma} \hat{c}^{\dagger}_{i\sigma}\hat{c}_{i\sigma} + U\, \hat{c}^{\dagger}_{i\uparrow}\hat{c}_{i\uparrow}\, \hat{c}^{\dagger}_{i\downarrow}\hat{c}_{i\downarrow} + \sum_{\mathbf{k}\sigma} \left(V_{\mathbf{k}i\sigma}\, \hat{c}^{\dagger}_{i\sigma}\hat{c}_{\mathbf{k}\sigma} + V^{*}_{i\mathbf{k}\sigma}\, \hat{c}^{\dagger}_{\mathbf{k}\sigma}\hat{c}_{i\sigma} \right) + \sum_{\mathbf{k}\sigma} \varepsilon^{(i)}_{\mathbf{k}\sigma}\, \hat{c}^{\dagger}_{\mathbf{k}\sigma}\hat{c}_{\mathbf{k}\sigma}. \tag{10}$$

The first two terms, those with the ε_i and U parameters, are the same as the local terms within the Anderson-Hubbard model (3). The third term represents a hybridization, i.e., a possibility of hopping the electron from the effective bath onto the site i-th with the amplitude (hybridization matrix element) $V_{\mathbf{k}i\sigma}$ and the reversed process. The last term describes a property of a single particle bath with a dispersion relation $\varepsilon^{(i)}_{\mathbf{k}\sigma}$. All creation and annihilation operators are fermionic for spin $1/2$ particles and $\mathbf{k}$ is a momentum corresponding to a referenced homogeneous lattice. We note that the SIAM Hamiltonian (10) is defined for each site i of the lattice, where the energies ε_i are different in principle. The hybridization $V_{\mathbf{k}i\sigma}$ and the dispersion relation $\varepsilon^{(i)}_{\mathbf{k}\sigma}$ are

not yet known and need to be derived self-consistently. Note that they are spin σ dependent when the magnetic systems are considered.
The common quantity that can be derived for the lattice problem (3) and for the SIAM Hamiltonian (10) are the diagonal and local Green functions, respectively,

$$G^{\mathrm{latt}}_{ij\sigma}(\omega) = -i\int d\omega\, e^{i\omega t}\big\langle T\hat{a}_{i\sigma}(t)\hat{a}^{\dagger}_{j\sigma}(0)\big\rangle \tag{11}$$

and

$$G^{\mathrm{imp}}_{ii\sigma}(\omega) = -i\int d\omega\, e^{i\omega t}\big\langle T\hat{c}_{i\sigma}(t)\hat{c}^{\dagger}_{i\sigma}(0)\big\rangle, \tag{12}$$

where t is a time and ω is a real frequency [20]. The self-consistency condition requires that both are the same, i.e.

$$G^{\mathrm{latt}}_{ii\sigma}(\omega) \overset{!}{=} G^{\mathrm{imp}}_{ii\sigma}(\omega) \equiv G_{i\sigma}(\omega). \tag{13}$$

The local Green function for the SIAM is given by

$$G^{\mathrm{imp}}_{ii\sigma}(\omega) = \frac{1}{\omega + \mu - \varepsilon_i - \varDelta_{i\sigma}(\omega) - \varSigma^{\mathrm{imp}}_{i\sigma}(\omega)}, \tag{14}$$

where

$$\varDelta_{i\sigma}(\omega) = \sum_{\mathbf{k}} \frac{|V_{\mathbf{k}i\sigma}|^2}{\omega - \varepsilon^{(i)}_{\mathbf{k}\sigma}} \tag{15}$$

is the so called hybridization function and $\varSigma_{i\sigma}(\omega)$ is the self-energy. When $U{=}0$ the self-energy vanishes. Similarly, the diagonal Green function for the lattice problem is given from the real-space Dyson equation

$$\big[G^{\mathrm{latt}}_{ij\sigma}(\omega)\big] = \Big[\big[G^{\mathrm{latt},0}_{ij\sigma}(\omega)\big]^{-1} - \varSigma_{ij\sigma}(\omega)\Big]^{-1}, \tag{16}$$

where $G^{\mathrm{latt},0}_{ij\sigma}(\omega)$ is the Green function for fermions on the lattice in the absence of interactions, i.e., $U{=}\,0$, and $\varSigma_{ij\sigma}(\omega)$ is the self-energy. Within the DMFT it is assumed, and shown to be exact in the infinite coordination number limit, that $\varSigma_{ij\sigma}(\omega) = \delta_{ij}\varSigma^{\mathrm{latt}}_{i\sigma}(\omega)$ is diagonal. For homogeneous systems, when the Fourier transform is applied, this condition is equivalent to the statement that the self-energy is momentum independent. The self-consistency condition (13) now takes the form

$$\varSigma^{\mathrm{latt}}_{i\sigma}(\omega) \overset{!}{=} \varSigma^{\mathrm{imp}}_{i\sigma}(\omega) \equiv \varSigma_{i\sigma}(\omega). \tag{17}$$

The set of equations (10)–(17) forms the **real-space dynamical mean-field theory** (R-DMFT) [21]. Determining self-consistently $\varSigma_{i\sigma}(\omega)$ together with $V_{\mathbf{k}i}$ and $\varepsilon^{i}_{\mathbf{k}}$ for each lattice site i allows us to determine all diagonal Green functions $G^{\mathrm{latt}}_{ii\sigma}(\omega)$ and other single-particle properties for a many-body lattice system.
The R-DMFT equations, though very general and applicable for homogeneous and for inhomogeneous lattices of any type, are difficult to use, in particular if the system size N_L is large. Indeed, if we deal with random inhomogeneities, the R-DMFT equations must be iterated for many realization of the disorder. It requires that the most difficult and time consuming part, the

SIAM problem (10) needs to be solved $N_L\times N_{\text{it}}\times N_{\text{dis}}$ times, where N_{it} is the number of iterations to get a self-consistency for a given realization of the disorder and N_{dis} is the number of disorder realizations. This obstacle motivates to search for an average description of the system, reintroducing back homogeneity and utilizing again the Fourier transformation between the real $\mathbf{R}_i$ and the reciprocal $\mathbf{k}$ spaces.

4 Averaged DMFT

In averaged descriptions of the system we need to take a statistical average of a physical observable on various realization of the quenched disorder. This will lead to the **averaged dynamical mean-field theory** (A-DMFT). On a one-particle level the spectral functions or the **density of states** (DOS) are such useful observables. The **local density of states** (LDOS) is defined as [20]

$$A_{i\sigma}(\omega) = -\frac{1}{\pi}\mathrm{Im}\, G_{i\sigma}(\omega+i0^+), \tag{18}$$

where now the Green function $G_{i\sigma}(\omega)$ is determined from the simplified SIAM, where the hybridization matrix and the bath dispersion relations are site independent, i.e.

$$\hat{H}_{\text{SIAM}} = \varepsilon_i\sum_{\sigma} \hat{c}^\dagger_{i\sigma}\hat{c}_{i\sigma} + U\,\hat{c}^\dagger_{i\uparrow}\hat{c}_{i\uparrow}\,\hat{c}^\dagger_{i\downarrow}\hat{c}_{i\downarrow} + \sum_{\mathbf{k}\sigma}\left(V_{\mathbf{k}\sigma}\,\hat{c}^\dagger_{i\sigma}\hat{c}_{\mathbf{k}\sigma} + V^*_{\mathbf{k}\sigma}\,\hat{c}^\dagger_{\mathbf{k}\sigma}\hat{c}_{i\sigma}\right) + \sum_{\mathbf{k}\sigma}\varepsilon_{\mathbf{k}\sigma}\,\hat{c}^\dagger_{\mathbf{k}\sigma}\hat{c}_{\mathbf{k}\sigma}. \tag{19}$$

Taking one of the generalized averages, the p-mean, we obtain the average density of states

$$A_\sigma(\omega) \equiv \left\langle A_{i\sigma}(\omega)\right\rangle_p = \left[\int d\varepsilon_i\, A_{i\sigma}(\omega)^p\, p(\varepsilon_i)\right]^{\frac{1}{p}}. \tag{20}$$

To recover the average Green function, needed to complete the self-consistency DMFT loop, we use the spectral representation theorem [20] and get

$$G_\sigma(\omega) \equiv \left\langle G_{i\sigma}(\omega)\right\rangle_p = \int d\omega' \frac{\langle A_{i\sigma}(\omega')\rangle_p}{\omega-\omega'}. \tag{21}$$

We note that for $p{=}1$-mean, i.e., arithmetic averaging, the Hilbert transform leads directly to

$$G^{\text{arith}}_\sigma(\omega) = \left\langle G_{i\sigma}(\omega)\right\rangle_{p=1} = \int d\varepsilon_i\, G_{i\sigma}(\omega)\, p(\varepsilon_i), \tag{22}$$

and the real and imaginary parts of the Green function can be averaged independently. For other p-means this linear property does not hold and one must explicitly use the Hilbert transform (21) as a step between.
We will be particularly interested in the geometric averaging when describing the Anderson localization. Then the averaging of the spectral function takes explicitly the form

$$A^{\text{geom}}_\sigma(\omega) \equiv \left\langle A_{i\sigma}(\omega)\right\rangle_{p=0} = e^{\int d\varepsilon_i \ln A_{i\sigma}(\omega)\, p(\varepsilon_i)}. \tag{23}$$

Now, since the average Green function is site independent, i.e., homogeneous, and the self-energy is uniform, i.e., site and $\mathbf{k}$ independent, we can use the Fourier transform and write the self-consistency condition that the average Green function $G_\sigma(\omega)$ and the one of the homogeneous system with the self-energy are equal, i.e.

$$G_\sigma(\omega) \stackrel{!}{=} \sum_{\mathbf{k}} \frac{1}{\omega - E_{\mathbf{k}} - \Sigma_\sigma(\omega)} = \frac{1}{\omega + \mu - \Delta_\sigma(\omega) - \Sigma_\sigma(\omega)}, \tag{24}$$

where $E_{\mathbf{k}}$ is the dispersion relation for the non-interacting particles in the reference homogeneous lattice, and the homogeneous hybridization function is

$$\Delta_\sigma(\omega) = \sum_{\mathbf{k}} \frac{|V_{\mathbf{k}\sigma}|^2}{\omega - \varepsilon_{\mathbf{k}\sigma}}. \tag{25}$$

Indeed, the equations (18)–(25) constitute a close set of the A-DMFT equations that can be solved iteratively until the self-consistency is reached. For systems without disorder this set of equations is exactly the same as in the standard DMFT.

5 DMFT and CPA

5.1 CPA for non-interacting systems

It is instructive to recover the standard CPA equation from the A-DMFT equations. When the system is non-interacting ($U=0$) the Hamiltonian (19) can be solved exactly, e.g., by means of the equations of motion, and we find that the local Green function is

$$G_{i\sigma}(\omega) = \frac{1}{\omega + \mu - \Delta_\sigma(\omega) - \varepsilon_i}\,. \tag{26}$$

The self-consistency equation (24) reads

$$G_\sigma(\omega) = \sum_{\mathbf{k}} \frac{1}{\omega - E_{\mathbf{k}} - \Sigma_\sigma(\omega)} = \int d\varepsilon_i \, \frac{1}{\omega + \mu - \Delta_\sigma(\omega) - \varepsilon_i}\, p(\varepsilon_i) \tag{27}$$

or

$$G_\sigma(\omega) = G_\sigma^{(0)}\big(\omega - \Sigma_\sigma(\omega)\big) = \int d\varepsilon_i \, \frac{1}{\omega + \mu - \Delta_\sigma(\omega) - \varepsilon_i}\, p(\varepsilon_i), \tag{28}$$

where

$$G_\sigma^{(0)}(\omega) = \sum_{\mathbf{k}} \frac{1}{\omega + \mu - E_{\mathbf{k}}} \tag{29}$$

is the Green function for non-interacting and homogeneous system. Using the RHS of the Eq. (24) we see that

$$G_\sigma^{(0)}\big(\omega - \Sigma_\sigma(\omega)\big) = \int d\varepsilon_i \, \frac{1}{\frac{1}{G_\sigma^{(0)}(\omega - \Sigma_\sigma(\omega))} - \big(\varepsilon_i - \Sigma_\sigma(\omega)\big)}\, p(\varepsilon_i), \tag{30}$$

and by arranging terms we finally get

$$\int d\varepsilon_i \, \frac{\varepsilon_i - \Sigma_\sigma(\omega)}{1 - \big(\varepsilon_i - \Sigma_\sigma(\omega)\big) G_\sigma^{(0)}\big(\omega - \Sigma_\sigma(\omega)\big)}\, p(\varepsilon_i) \equiv \int d\varepsilon_i T_{ii\sigma}(\omega)\, p(\varepsilon_i) = 0, \tag{31}$$

where the T-matrix

$$T_{ii\sigma}(\omega) = \frac{\varepsilon_i - \Sigma_\sigma(\omega)}{1 - \big(\varepsilon_i - \Sigma_\sigma(\omega)\big) G^{(0)}_\sigma\big(\omega - \Sigma_\sigma(\omega)\big)} \tag{32}$$

describes multiple-scattering processes on the i-th impurity site with an effective potential $\varepsilon_i - \Sigma_\sigma(\omega)$. This is exactly the CPA self-consistency equation on vanishing of the average T-matrix defined with respect to the mean environment. Thus we see that the A-DMFT with p=1-mean, arithmetic averaging, reduces to the coherent potential approximation in the noninteracting limit.

5.2 Binary alloys and alloy band splitting

In a binary alloy, two different atoms are distributed randomly on lattice sites. It is modeled by assuming that one of the atom has an atomic energy $\varepsilon_A = -\Delta/2$ and the other $\varepsilon_B = \Delta/2$, $\Delta \geq 0$. Since they are distributed randomly the probability distribution function takes the form

$$p(\varepsilon) = x_A \delta(\varepsilon - \varepsilon_A) + x_B \delta(\varepsilon - \varepsilon_B), \tag{33}$$

where $x_A = N_A/N_L$ and $x_B = N_B/N_L$ are the concentrations of the A and B atoms, respectively. Note, $x_A + x_B = 1$. This binary alloy distribution is very special: only two energies are allowed. It leads to the alloy-band splitting. Namely, from the localization theorem (the Hadamard-Gerschgorin theorem in matrix algebra) it is known that if the Hamiltonian (3), with the binary alloy distribution for ε_i, is bounded, then there is a gap in the single particle spectrum for sufficiently large $\Delta \gg \max\big(|t|, U\big)$ [4]. Hence, at $\Delta = \Delta_c$ the DOS splits into two parts corresponding to the lower and the upper alloy subbands with centers of masses at the ionic energies ε_A and ε_B, respectively. The width of the alloy gap is of the order Δ. The lower and the upper alloy subband contains $2x_A N_L$ and $2x_B N_L$ states, respectively. For convenience, we note $x_A = x$ and $x_B = 1-x$, where $0 \leq x \leq 1$. A simplified proof of that fact is given in Appendix A and actually does not rely on an averaging approximation, like the CPA.

5.3 Mott-Hubbard transition at fractional filling in the binary alloy disordered Hubbard model

The Mott-Hubbard metal-insulator transition occurs upon increasing the interaction strength U in the simple Hubbard models (3) if the number of electrons N_e is commensurate with the number of lattice sites N_L or, more precisely, if the ratio N_e/N_L is an odd integer. At zero temperature it is a continuous transition whereas at finite temperatures the transition is of the first order [13]. The transition happens by a dynamical redistribution of the spectral weight such that two Hubbard subbands are formed and a central, quasiparticle peak in between, which vanishes at the critical interaction $U = U_c$ where the system becomes a Mott insulator.

Surprisingly, in the presence of binary alloy disorder the MIT occurs at fractional filling [22]. We describe this situation by using the Anderson-Hubbard model (3) with the distribution (33), which corresponds to a binary-alloy system composed of two different atoms A and B. As

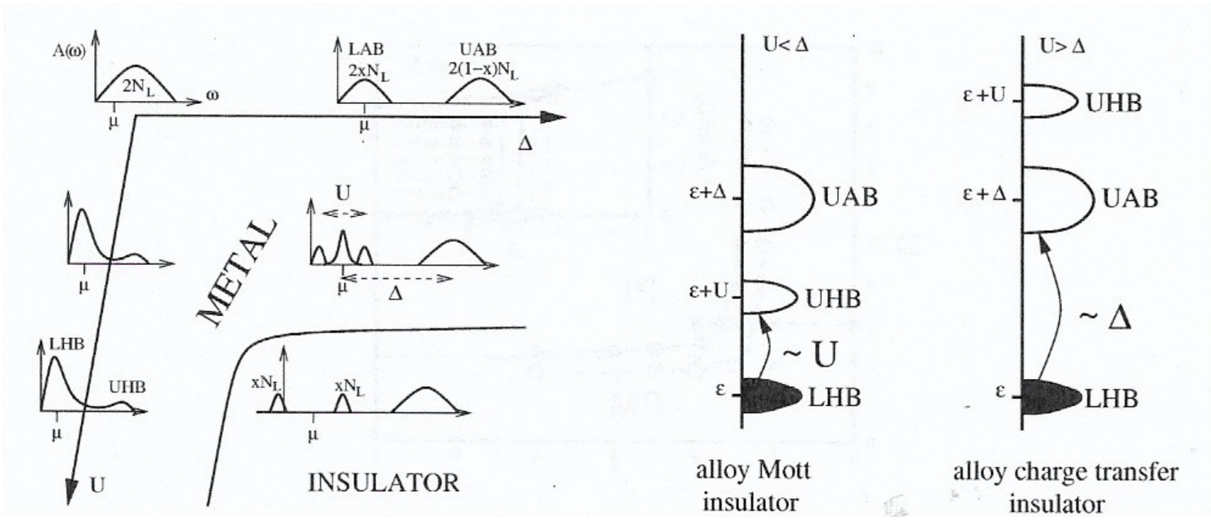

Fig. 1: *Left: Schematic plot representing the Mott-Hubbard metal-insulator transition in a correlated electron system with binary alloy disorder. The shapes of DOS are shown for different interactions U and disorder strengths Δ. Increasing Δ at $U\!=\!0$ leads to splitting of the spectral function into the lower (LAB) and the upper (UAB) alloy subbands, which contains $2xN_L$ and $2(1-x)N_L$ states, respectively. Increasing U at $\Delta = 0$ leads to the occurrence of lower (LHB) and upper (UHB) Hubbard subbands. The Fermi energy for filling $n = x$ is indicated by μ. At $n = x$ (or $n = 1+x$, not shown in the plot) the LAB (UAB) is half-filled. In this case an increase in U and Δ leads to the opening of a correlation gap at the Fermi level and the system becomes a Mott insulator. Right: Two possible insulating states in the correlated electron system with binary-alloy disorder. When $U < \Delta$ the insulating state is an alloy Mott insulator with an excitation gap in the spectrum of the order of U. When $U > \Delta$ the insulating state is an alloy charge transfer insulator with an excitation gap of the order of Δ; after Ref. [22].*

discussed there is a binary alloy band splitting expected for large Δ. New possibilities appear in systems with correlated electrons and binary alloy disorder [22]. The Mott-Hubbard metal-insulator transition can occur at any filling $n = N_e/N_L = x$ or $1+x$, corresponding to a half-filled lower or to a half-filled upper alloy subband, respectively, as shown schematically for $n = x$ in Fig. 1.

The Mott insulator can then be approached either by increasing U when $\Delta \geq \Delta_c$ (alloy band splitting limit), or by increasing Δ when $U \geq U_c$ (Hubbard band splitting limit). The nature of the Mott insulator in the binary alloy system can be understood physically as follows. Due to the high energy cost of the order of U the randomly distributed ions with lower (higher) local energies ε_i are singly occupied at $n = x$ ($n = 1+x$), i.e., the double occupancy is suppressed. In the Mott insulator with $n = x$ the ions with higher local energies are empty and do not contribute to the low-energy processes in the system. Likewise, in the Mott insulator with $n = 1+x$ the ions with lower local energies are double occupied implying that the lower alloy subband is blocked and does not play any role.

For $U > Uc(\Delta)$ in the Mott insulating state with binary alloy disorder one may use the lowest excitation energies to distinguish two different types of insulators. Namely, for $U < \Delta$ an excitation must overcome the energy gap between the lower and the upper Hubbard subbands,

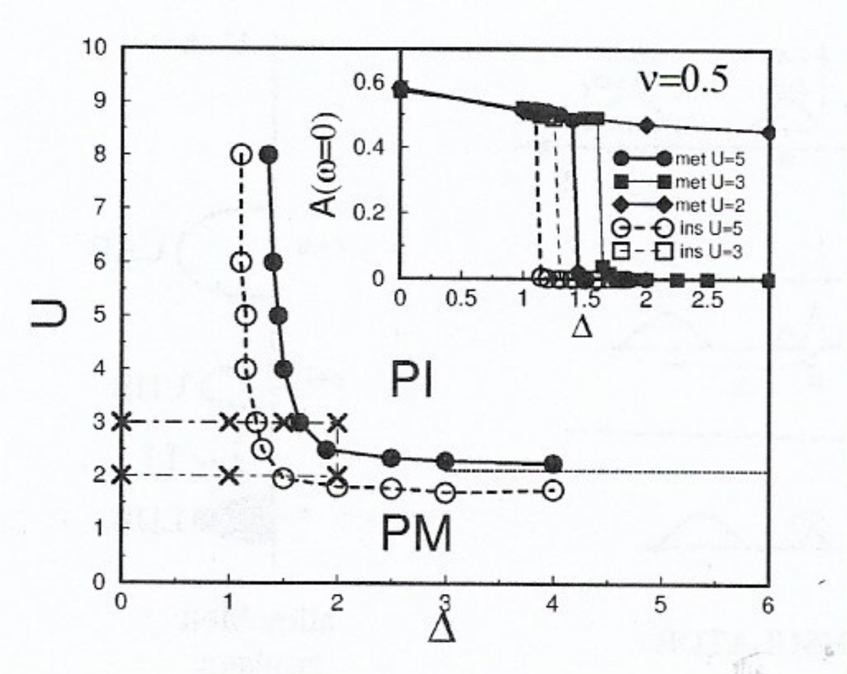

Fig. 2: *Ground state phase diagram of the Hubbard model with binary-alloy disorder at filling $n{=}x{=}0.5$. The filled (open) dots represent the boundary between paramagnetic metallic (PM) and paramagnetic insulating (PI) phases as determined by DMFT with the initial input given by the metallic (insulating) hybridization function. The horizontal dotted line represents U_c obtained analytically from an asymptotic theory in the limit $\Delta \to \infty$. Inset: hysteresis in the spectral functions at the Fermi level obtained from DMFT with an initial metallic (insulating) host represented by filled (open) symbols and solid (dashed) lines; after Ref. [22].*

as indicated in Fig. 1. We call this insulating state an *alloy Mott insulator*. On the other hand, for $\Delta < U$ an excitation must overcome the energy gap between the lower Hubbard subband and the upper alloy-subband, as shown in Fig. 1. We call this insulating state an *alloy charge transfer insulator*.

In Fig. 2 we present a particular phase diagram for the Anderson-Hubbard model at filling $n = 0.5$ showing a Mott-Hubbard type of MIT with a typical hysteresis.

5.4 Ferromagnetism in the binary alloy disordered Hubbard model; disorder-induced enhancement of the Curie temperature

Itinerant ferromagnetism in the pure Hubbard model occurs only away from half-filling and if the DOS is asymmetric and peaked at the lower edge [23, 24]. While the Curie temperature T_c increases with the strength of the electron interaction one would expect it to be lowered by disorder. However, our investigations show that in some cases the Curie temperature can actually be increased by binary alloy disorder [25,26].

Indeed, the Curie temperature as a function of alloy concentration exhibits a very rich and interesting behavior as is shown in Fig. 3. At some concentrations and certain values of U, Δ, and n, the Curie temperature is enhanced above the corresponding value for the non-disordered case ($x{=}\,0$ or 1). This is shown in the upper part of Fig. 3 for $0 < x < 0.2$. The relative increase in T_c can be as large as 25%, as is found for $x \approx 0.1$ at $n = 0.7$, $U = 2$ and $\Delta = 4$.

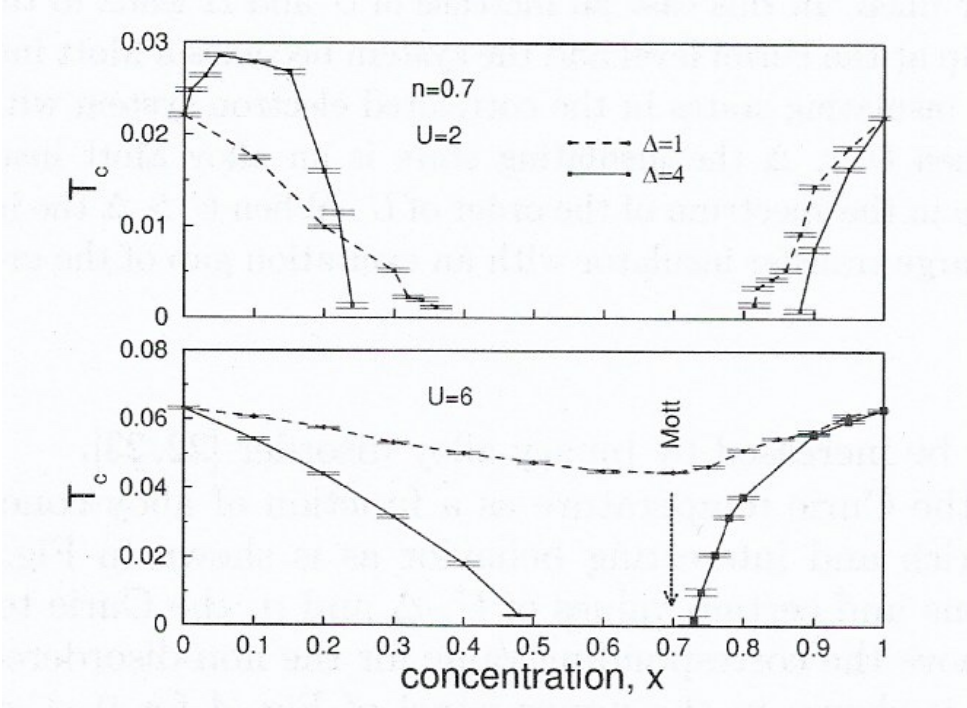

Fig. 3: *Curie temperature as a function of alloy concentration x at $U = 2$ (upper part) and 6 (lower part) for $n = 0.7$ and disorder $\Delta = 1$ (dashed lines) and 4 (solid lines); after Refs. [25, 26]. Temperatures are in the energy units.*

This unusual enhancement of T_c is caused by three distinct features of interacting electrons in the presence of binary alloy disorder:

i) The Curie temperature in the non-disordered case $T_c^p \equiv T_c(\Delta{=}0)$, depends non-monotonically on band filling n [24]. Namely, $T_c^p(n)$ has a maximum at some filling $n = n^*(U)$, which increases as U is increased; see also our schematic plots in Fig. 4.

ii) As described above, in the alloy-disordered system the band is split when $\Delta \gg \max(|t|, U)$. As a consequence, for $n < 2x$ and $T \ll \Delta$ electrons occupy only the lower alloy subband and for $n > 2x$ both the lower and upper alloy subbands are filled. In the former case the upper subband is empty while in the latter case the lower subband is completely full. Effectively, one can therefore describe this system by a Hubbard model mapped onto either the lower or the upper alloy subband, respectively. The second subband plays a passive role. Hence, the situation corresponds to a single band with the effective filling $n_{\text{eff}} = n/x$ for $n < 2x$ and $n_{\text{eff}} = (n{-}2x)/(1{-}x)$ for $n > 2x$. It is then possible to determine T_c from the phase diagram of the Hubbard model without disorder.

iii) The disorder leads to a reduction of $T_c^p(n_{\text{eff}})$ by a factor $\alpha = x$ if the Fermi level is in the lower alloy subband or $\alpha = 1{-}x$ if it is in the upper alloy subband, i.e., we find

$$T_c(n) \approx \alpha T_c^p(n_{\text{eff}}), \tag{34}$$

when $\Delta \gg \max(|t|, U)$. Hence, as illustrated in Fig. 4, T_c can be determined by $T_c^p(n_{\text{eff}})$. Surprisingly, then, it follows that for suitable U and n the Curie temperature of a disordered system can be higher than that of the corresponding non-disordered system.

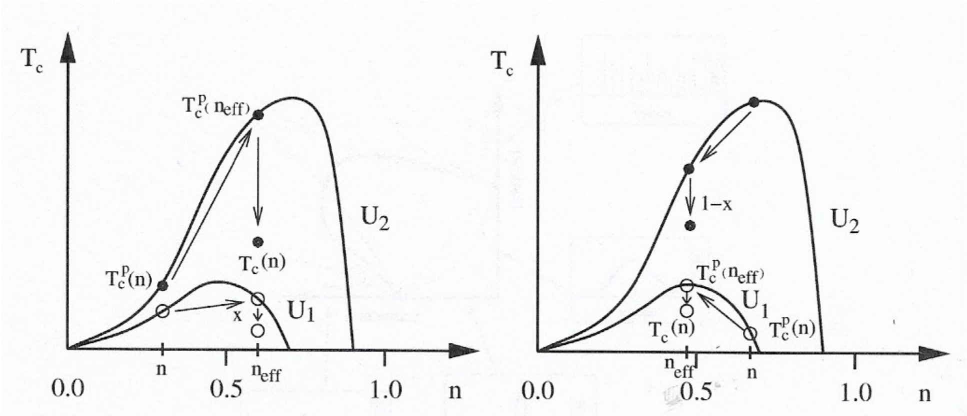

Fig. 4: *Schematic plots explaining the filling dependence of T_c for interacting electrons with strong binary alloy disorder. Curves represent T_c^p, the Curie temperature for the pure system, as a function of filling n at two different interactions $U_1 \ll U_2$. Left: For $n < x$, T_c of the disordered system can be obtained by transforming the open (for U_1) and the filled (for U_2) point from n to $n_{eff} = n/x$, and then multiplying $T_c^p(n/x)$ by x as indicated by arrows. One finds $T_c(n) < T_c^p(n)$ for U_1, but $T_c(n) > T_c^p(n)$ for U_2. Right: For $n > x$, T_c of the disordered system can be obtained by transforming $T_c^p(n)$ from n to $n_{eff} = (n-2x)/(1-x)$, and then multiplying $T_c^p[(n-2x)/(1-x)]$ by $1-x$ as indicated by arrows. One finds $T_c(n) > T_c^p(n)$ for U_1, but $T_c(n) < T_c^p(n)$ for U_2; after Refs. [25, 26].*

6 DMFT and TMT

6.1 Typical medium theory for Anderson localization

The Mott-Hubbard MIT is caused by the Coulomb correlations in the pure system. By contrast, the Anderson MIT, also referred to as the Anderson localization, is due to coherent backscattering from randomly distributed impurities in a system without interaction [5]. It is therefore a challenge to investigate the effect of the simultaneously presence of interactions and disorder on electronic systems [27, 28]. In particular, the question arises whether it will suppress or enlarge a metallic phase. And what about the Mott and Anderson insulating phases: will they be separated by a metallic phase? Possible scenarios are schematically plotted in Fig. 5.

The Mott-Hubbard MIT is characterized by the opening of a gap in the density of states at the Fermi level. At the Anderson localization transition the character of the spectrum at the Fermi level changes from a continuous spectrum to a dense, pure point spectrum. It is plausible to assume that both MITs can be characterized by a single quantity, namely, the local density of states. Although the LDOS is not an order parameter associated with a symmetry breaking phase transition, it discriminates between a metal and an insulator, which is driven by correlations and disorder, cf. insets to Fig. 5.

In a disordered system the LDOS depends on a particular realization of the disorder in the system. To obtain a full understanding of the effects of disorder it would therefore in principle be necessary to determine the entire probability distribution function of the LDOS, which is almost never possible. Instead one might try to calculate moments of the LDOS. This, however, is insufficient because the arithmetically averaged LDOS (first moment) stays finite at the Anderson MIT [29]. It was already pointed out by Anderson [5] that the *typical* values of random quanti-

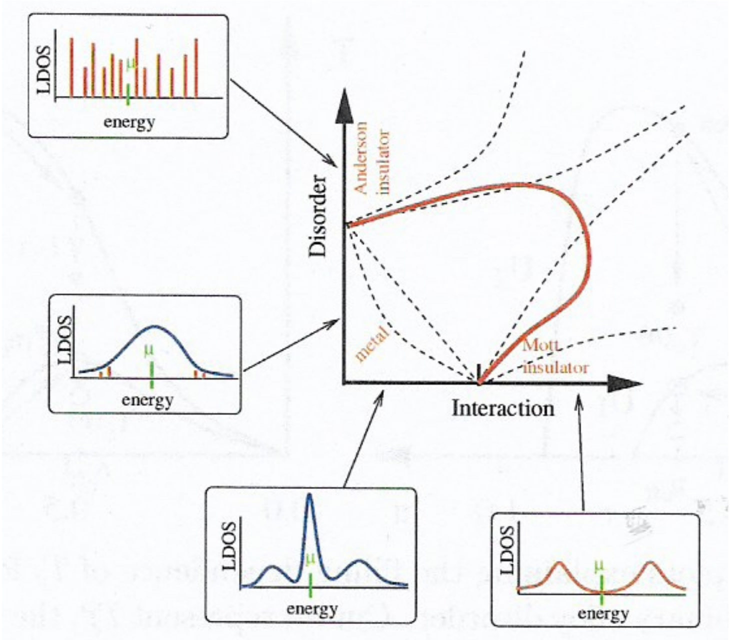

Fig. 5: *Possible phases and phase transitions triggered by interaction and disorder in the same system. According to DMFT investigations the simultaneous presence of correlations and disorder enhances the metallic regime (thick line); the two insulating phases are connected continuously. Insets show the local density of states when disorder or interaction is switched off.*

ties, which are mathematically given by the most probable values of the probability distribution functions, should be used to describe localization. The geometrical mean gives an approximation of the most probable (*typical*) value of the LDOS and vanishes at a critical strength of the disorder, hence providing an explicit criterion for the Anderson localization [5, 30, 31].

In the following we will use the simple box probability distribution function of the on-site random energies ε_i, i.e.

$$p(\varepsilon_i) = \begin{cases} \frac{1}{\Delta} & \text{for } |\varepsilon_i| \leq \Delta \\ 0 & \text{otherwise.} \end{cases} \tag{35}$$

Other types of the continuous probability distribution functions would lead to the same generic results although detailed numbers might be different. The reason is that this probability distribution does not yield any alloy band splitting.

6.2 Anderson localization in disordered Hubbard and Falicov-Kimball models

A non-perturbative framework for investigations of the Mott-Hubbard MIT in lattice electrons with a local interaction and disorder is provided by the DMFT [13]. If in this approach the effect of local disorder is taken into account through the arithmetic mean of the LDOS [32, 33] one obtains, in the absence of interactions, the well-known coherent potential approximation (CPA) [36], which does not describe the physics of Anderson localization. To overcome this deficiency Dobrosavljević *et al.* [31] incorporated the geometrically averaged LDOS into the self-consistency cycle and thereby derived a mean-field theory of Anderson localization which

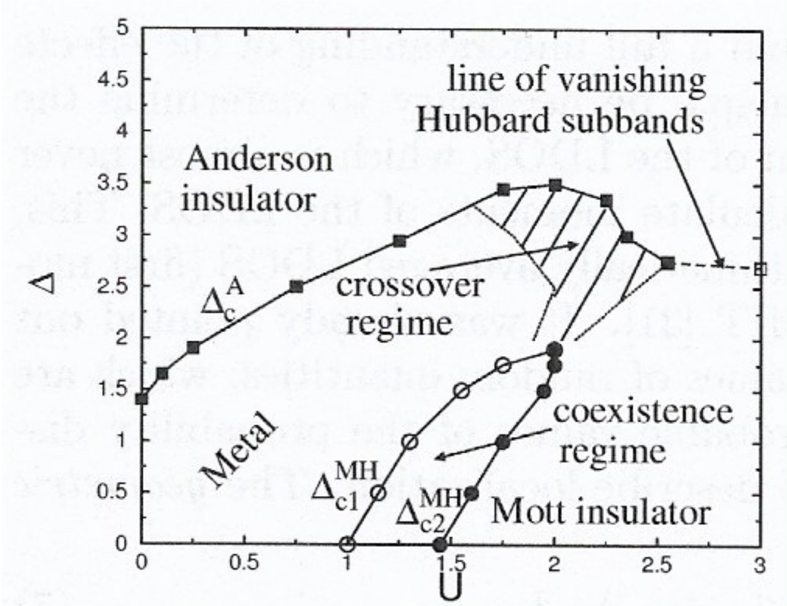

Fig. 6: *Non-magnetic ground state phase diagram of the Anderson-Hubbard model at half-filling as calculated by DMFT with the typical local density of states; after Refs. [27].*

reproduces many of the expected features of the disorder-driven MIT for non-interacting electrons. This scheme uses only one-particle quantities and is therefore easily incorporated into the DMFT for disordered electrons in the presence of phonons [34], or Coulomb correlations [27, 28]. In particular, the DMFT with geometrical averaging allows to compute phase diagrams for the Anderson-Hubbard model (3) and the Anderson-Falicov-Kimball model (4) with the continuous probability distribution function at half-filling [27, 28]. In this way we found that, although in both models the metallic phase is enhanced for small and intermediate values of the interaction and disorder, metallicity is finally destroyed. Surprisingly, the Mott and Anderson insulators are found to be continuously connected. Phase diagrams for the non-magnetic ground state are shown in Fig. 6 for the Anderson-Hubbard model and in Fig. 7 for the Anderson-Falicov-Kimball model.

7 Outlook

In these lecture notes we have seen that a combination between the correlations of interacting electrons and disorder leads to novel and unexpected possibilities. And the combination of the DMFT with statistical methods to treat randomness has turned out to be very successful in describing the correlated electrons with disordered potentials. Continuation of this research turns in many directions.

The influence of non-uniform or random external potentials on the existence and stability of the antiferromagnetic phases in the Hubbard model was investigated in Ref. [21, 35]. The study of the Anderson transition in the presence of binary-alloy disorder was performed in [36]. The same type of disorder was used to study ferromagnetism in the periodic Anderson model in [37]. A spin-selective disorder and the localization MITs were investigated in [38, 39]. More

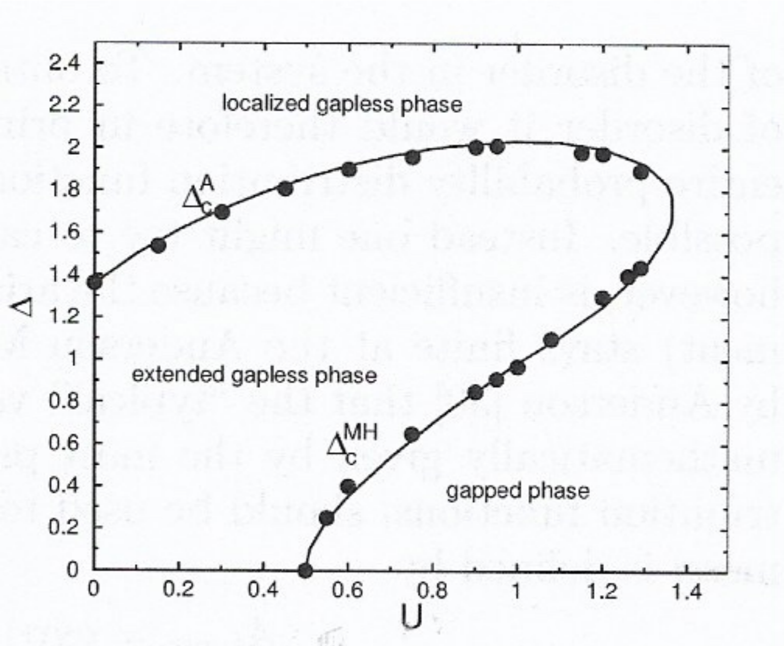

Fig. 7: *Non-magnetic ground state phase diagram of the Anderson-Falicov-Kimball model at half-filling as calculated by DMFT with the typical local density of states; after Refs. [28].*

recently, the typical medium theory was extended to treat systems with off-diagonal, hopping disorder [40].

In conclusion, the dynamical mean-field theory for correlated electrons with disorder is a well established method to comprehensively describe interacting electrons on crystal lattices or even fermionic atoms on optical lattices.

Acknowledgment

The author thanks Dieter Vollhardt for the fruitful quarter-century collaboration on correlated lattice systems with disorder. He also thanks Walter Hofstetter for a long collaboration on this subject. He also acknowledges Liviu Chioncel, Denis Semmler, Jan Skolimowski, Martin Ulmke, and Unjong Yu for various collaborations. The Appendix A is based on the notes from Bedrich Velicky, received in 2001.

A Proof of the alloy band splitting theorem

In order to prove the alloy band splitting theorem we need to show firstly the so called localization theorem. For that we assume that the unperturbed Hamiltonian $\hat{H}_0$ has a point like spectrum, i.e.

$$\hat{H}_0 = \sum_i \varepsilon_i |i\rangle\langle i|, \tag{36}$$

where ε_i are real discrete eigenvalues of the Hamiltonian $\hat{H}_0$ in the $\{|i\rangle\}$ base. Any normalized vector can be expanded in this basis

$$|\alpha\rangle = \sum_i c_i |i\rangle, \tag{37}$$

with $\|\alpha\|^2 \equiv |\langle\alpha|\alpha\rangle|^2 = \sum_i |c_i|^2 = 1$. Now we add a perturbation $\hat{T}$ to our Hamiltonian

$$\hat{H} = \hat{H}_0 + \hat{T}, \tag{38}$$

such that the perturbation part $\hat{T}$ is bounded, i.e., for any normalized vector $|\alpha\rangle$ we have that

$$\|\hat{T}\| \equiv \langle\alpha|\hat{T}|\alpha\rangle < \infty. \tag{39}$$

We also define a *distance* of the complex number λ from the spectrum of $\hat{H}_0$ Hamiltonian as

$$d(\lambda) = \inf\big\{|\lambda - \varepsilon_i|\big\}. \tag{40}$$

We can easily show that $d(E) \leq \|\hat{T}\|$ where $\hat{H}|\alpha\rangle = E|\alpha\rangle$, i.e., the distance between the spectra points of the full Hamiltonian $\hat{H}$ and the unperturbed Hamiltonian $\hat{H}_0$ is bounded: Indeed, from $(E - \hat{H}_0)|\alpha\rangle = \hat{T}|\alpha\rangle$ we get that $\langle\alpha|(E - \hat{H}_0)^2|\alpha\rangle = \langle\alpha|\hat{T}^2|\alpha\rangle$ or, equivalently, $\sum_i |c_i|^2 (E - \varepsilon_i)^2 = \|\hat{T}\|^2$. Estimating the left hand side by $\sum_i |c_i|^2 (E - \varepsilon_i)^2 \geq d(E)^2 \sum_i |c_i|^2 = d(E)^2$ we obtain the inequality $d(E) \leq \|\hat{T}\|$. This results is known as a *localization theorem.* In particular, it follows that the spectrum of $\hat{H}$ is covered by the union of spectra sets

$$\mathcal{A} = \bigcup_i \big\langle \varepsilon_i - \|\hat{T}\|, \varepsilon_i + \|\hat{T}\| \big\rangle. \tag{41}$$

If the perturbation Hamiltonian $\hat{T} = \sum_{ij} t_{ij}\, \hat{a}_i^\dagger \hat{a}_j$ is a tight-binding Hamiltonian on a uniform lattice, diagonalized by the Fourier transform to the form $\hat{T} = \sum_{\mathbf{k}} E_{\mathbf{k}}\, \hat{a}_{\mathbf{k}}^\dagger \hat{a}_{\mathbf{k}}$, with the dispersion $E_{\mathbf{k}}$, the spectrum of $\hat{T}$ is bounded between $t_{\text{min}} = \min(E_{\mathbf{k}})$ and $t_{\text{max}} = \max(E_{\mathbf{k}})$. Therefore, we get the estimate for the spectrum of $\hat{H}$

$$\mathcal{A} = \bigcup_i \big\langle \varepsilon_i - t_{\text{min}}, \varepsilon_i + t_{\text{max}} \big\rangle. \tag{42}$$

As a consequence, for a binary alloy systems ($i = A$ or B)

$$\mathcal{A} = \big\langle \varepsilon_A - t_{\text{min}}, \varepsilon_A + t_{\text{max}} \big\rangle \cup \big\langle \varepsilon_B - t_{\text{min}}, \varepsilon_B + t_{\text{max}} \big\rangle, \tag{43}$$

or in our binary alloy model

$$\mathcal{A} = \left\langle -\frac{\Delta}{2} - t_{\text{min}}, -\frac{\Delta}{2} + t_{\text{max}} \right\rangle \cup \left\langle \frac{\Delta}{2} - t_{\text{min}}, \frac{\Delta}{2} + t_{\text{max}} \right\rangle. \tag{44}$$

If $|t_{\text{max}} - t_{\text{min}}| < \Delta$ the band is split and two separated alloy subbands are formed [4].

References

[1] H. Weyl, *Symmetries* (Princeton University Press, 1952)

[2] Lao Tzu, *Tao teh ching* (St. John's University Press, New York 1961)

[3] R. Zallen, *The physics of amorphous solids* (Wiley, 1983)

[4] J.M. Ziman, *Models of disorders* (Cambridge University Press, 1979)

[5] P.W. Anderson, Phys. Rev. **109**, 1492 (1958)

[6] `https://en.wikipedia.org/wiki/Central_limit_theorem`

[7] R. Brout: *Statistical Mechanical Theory of a Random Ferromagnetic System*, Phys. Rev. **115**, 824, (1959)

[8] G. Schubert, J. Schleede, K. Byczuk, H. Fehske, and D. Vollhardt, Phys. Rev. B **81**, 155106 (2010)

[9] M. de Carvalho: *Mean, What do You Mean?*, Am. Stat. **70**, 270 (2016)

[10] E.L. Crow and K. Shimizu (eds.): *Log-normal distribution - theory and applications* (Dekker, 1988)

[11] E.W Montroll and M.F. Schlesinger, J. Stat. Phys. **32**, 209 (1983)

[12] R.J. Elliot, J.A. Krumhansl, and P.L. Leath, Rev. Mod. Phys. **46**, 465 (1974)

[13] D. Vollhardt, in V.J. Emery (ed.): *Correlated Electron Systems* (World Scientific, 1993), p. 57; Th. Pruschke, M. Jarrell, J.K. Freericks, Adv. Phys. **44**, 187 (1995); A. Georges, G. Kotliar, W. Krauth, and M.J. Rozenberg, Rev. Mod. Phys. **68**, 13 (1996)

[14] G. Baym and L. Kadanoff, Phys. Rev. **124**, 287 (1961); G. Baym, Phys. Rev. **127**, 836 (1962)

[15] W. Metzner and D. Vollhardt, Phys. Rev. Lett. **62**, 1066 (1989)

[16] D. Vollhardt, in E. Pavarini, E. Koch, D. Vollhardt, and A. Lichtenstein (eds.): *The LDA+DMFT approach to strongly correlated electrons*, Modeling and Simulations, Vol. 1 (Forschungszentrum Jülich, 2011)

[17] M. Kollar, in E. Pavarini, E. Koch, D. Vollhardt, and A. Lichtenstein (eds.): *The LDA+DMFT approach to strongly correlated electrons*, Modeling and Simulations, Vol. 1 (Forschungszentrum Jülich, 2011)

[18] D. Vollhardt: in E. Pavarini, E. Koch, A. Lichtenstein, and D. Vollhardt (eds.): *DMFT: From Infinite Dimensions to Real Materials*, Modeling and Simulations, Vol. 8 (Forschungszentrum Jülich, 2018)

[19] M. Kollar: in E. Pavarini, E. Koch, A. Lichtenstein, and D. Vollhardt (eds.): *DMFT: From Infinite Dimensions to Real Materials*, Modeling and Simulations, Vol. 8 (Forschungszentrum Jülich, 2018)

[20] J.W. Negele and H. Orland, *Quantum many-particle systems*, (Perseus, 1988)

[21] M. Snoek, I. Titvinidze, C. Toke, K. Byczuk, and W. Hofstetter, New J. Phys. **10**, 093008 (2008)

[22] K. Byczuk, W. Hofstetter, and D. Vollhardt, Phys. Rev. B **69**, 045112 (2004)

[23] M. Ulmke, Eur. Phys. J. B **1**, 301 (1998)

[24] J. Wahle, N. Blümer, J. Schlipf, K. Held, D. Vollhardt, Phys. Rev. B **58**, 12749 (1998)

[25] K. Byczuk, M. Ulmke, D. Vollhardt, Phys. Rev. Lett. **90**, 196403 (2003)

[26] K. Byczuk, M. Ulmke, Eur. Phys. J. B **45**, 449 (2005)

[27] K. Byczuk, W. Hofstetter, D. Vollhardt, Phys. Rev. Lett. **94**, 056404 (2005)

[28] K. Byczuk, Phys. Rev. B **71**, 205105 (2005)

[29] D. Lloyd, J. Phys. C **2**, 1717 (1969); D. Thouless, Phys. Rep. **13**, 93 (1974); F. Wegner, Z. Phys. B **44**, 9 (1981)

[30] V. Dobrosavljević, G. Kotliar, Phys. Rev. Lett. **78**, 3943 (1997)

[31] V. Dobrosavljević, A.A. Pastor, B.K. Nikolić, Europhys. Lett. **62**, 76 (2003)

[32] V. Janiš, D. Vollhardt, Phys. Rev. B **46**, 15712 (1992); M. Ulmke, V. Janiš, D. Vollhardt, Phys. Rev. B **51**, 10411 (1995)

[33] R. Vlaming, D. Vollhardt, Phys. Rev. B **45**, 4637 (1992)

[34] F.X. Bronold, A. Alvermann, H. Fehske, Philos. Mag. **84**, 637 (2004)

[35] K. Byczuk, W. Hofstetter, and D. Vollhardt, Phys. Rev. Lett. **102**, 146403 (2009)

[36] D. Semmler, K. Byczuk, and W. Hofstetter, Phys. Rev. B **81**, 115111 (2010)

[37] U. Yu, K. Byczuk, and D. Vollhardt, Phys. Rev. Lett. 100, 246401 (2008)

[38] K. Makuch, J. Skolimowski, P.B. Chakraborty, K. Byczuk, and D. Vollhardt, New J. Phys. **15**, 045031 (2013)

[39] J. Skolimowski, K. Byczuk, and D. Vollhardt, Phys. Rev. B **92**, 094202 (2015); J. Phys. Commun. **2**, 025031 (2018)

[40] A. Weh, Y. Zhang, A. Östlin, H. Terletska, D. Bauernfeind, K. -M. Tam, H.G. Evertz, K. Byczuk, D. Vollhardt, and L. Chioncel, Phys. Rev. B **104**, 045127 (2021)